ELSEVIER

Journal of Nuclear Materials 307–311 (2002) 1282–1288

journal of nuclear materials

www.elsevier.com/locate/jnucmat

Improvement of the thermo-mechanical properties of fine grain graphite by doping with different carbides

C. García-Rosales [a,*], N. Ordás [a], E. Oyarzabal [a], J. Echeberria [a], M. Balden [b], S. Lindig [b], R. Behrisch [b]

[a] *Centro de Estudios e Investigaciones Técnicas de Gipuzkoa (CEIT) and Escuela Superior de Ingenieros, Universidad de Navarra, Po Manuel Lardizabal 15, P.O. Box 1555, Basque Country, E-20009 San Sebastián, Spain*

[b] *Max-Planck-Institut für Plasmaphysik, EURATOM Association, Boltzmannstr. 2, D-85748 Garching, Germany*

Abstract

The possibilities for optimization of doped fine grain graphites with high thermal conductivity and high thermal shock resistance are demonstrated at laboratory scale. A mixture of MCMB powder and different carbides (B_4C, TiC, VC, ZrC and WC) was used as starting material. VC acts as catalyst of the graphitization at the lowest temperature, and ZrC is the most effective catalyst of all investigated carbides. A direct proportionality between the mean crystallite height, L_c, and the thermal conductivity at room temperature was found for all materials except for the B_4C- and the ZrC-doped graphites. With increasing graphitization temperature the open porosity of all doped materials becomes gradually closed, suggesting the existence of a diffusion mechanism responsible for both the catalytic effect and the closing of the open porosity. The addition of carbides does not strongly influence the mechanical properties of pure graphite. A high ratio flexural strength to Young's modulus was achieved.

1. Introduction

Carbon materials are candidates for those areas of the vessel wall of fusion devices receiving the highest power densities. One critical point for the application of these materials is their chemical sputtering under hydrogen bombardment from the plasma, leading to enhanced erosion and contributing to a high tritium inventory in redeposited carbon layers [1,2]. Doping of carbon with small amounts (several at.%) of some elements like B, Si, Ti or W is known to reduced one or both processes of chemical erosion. This reduction will be the more effective, the finer and more homogeneously the dopants are distributed in the graphite matrix [3]. Other important properties, however, with regard to the application of doped carbon materials for limiters and divertor plates are also the thermal conductivity, which should be as high as possible to allow fast heat transfer, and the thermo-mechanical properties (high strength, low Young's modulus) in view of a high thermal shock resistance. These properties can be improved by proper selection of the dopants, by using starting powders with very small particle size and particle size distribution, and by a rigorous control of all manufacturing steps [3].

This work demonstrates at laboratory scale the development possibilities for optimization of doped isotropic fine grain graphites with high thermal conductivity and high thermal shock resistance, to make them competitive with other first wall candidate materials for fusion devices.

2. Experimental

The starting carbon material consists of a self-sintering powder of meso-carbon microbeads (MCMB) based on petroleum residues produced in a semi-industrial plant by the Spanish company REPSOL-YPF. The

* Corresponding author. Tel.: +34-943 21 28 00; fax: +34-943 21 30 76.

E-mail address: cgrosales@ceit.es (C. García-Rosales).

0022-3115/02/$ - see front matter
PII: S0022-3115(02)00960-1

MCMB powder was jet-milled, after which it showed a bimodal particle size distribution with a mean particle size around 2.6 μm.

As dopants, the following carbides were used: B_4C, TiC, VC, ZrC and WC. These carbides show a catalytic effect on the graphitization [4], which is important in view of improving the thermal conductivity of the final material. They are stable up to very high temperatures, have a relatively low vapor pressure and most of them show a relatively wide homogeneity range [5]. The metals were selected so that they cover a wide range in atomic mass. The mean particle size of the carbide powders was ~1 μm except for the WC powder (~0.7 μm). The VC powder has a relatively high oxygen content (~5 wt%), which will be released during the first graphitization steps and has to be taken into account. The carbides were added to the carbon powder up to a metal concentration of ~4 at.%. This concentration was corroborated after graphitization by Rutherford backscattering for some of the samples.

After mixing, the powders were molded uni-axially at 150 MPa to cylindrical bodies (16 mm $\varnothing \times \sim 5$ mm height) and beams ($55 \times 15 \times \sim 5$ mm^3). Calcination was performed at 1000 °C in nitrogen atmosphere. The graphitization treatments were preformed in a graphite resistance furnace in He atmosphere at temperatures up to 2900 °C. The total mass loss of the material without carbides during heat treatment ($\Delta m/m$) was ~13%.

After calcination and graphitization the bulk density and the open porosity of all samples, and the true density of the undoped material were measured. The bulk density was determined geometrically, while the true density and the open porosity were measured with a He pycnometer. The total porosity was calculated from the bulk and true densities.

After graphitization, the crystallite size perpendicular to the graphite basal planes, L_c, was measured for all samples by X-ray diffraction from the width of the (0 0 2) reflex. This parameter is a good indicator of the graphitization degree of the carbon in the samples [6].

The thermal diffusivity of a few samples after some graphitization cycles was measured by the laser-flash method over the temperature range 20–1200 °C, and for two samples also down to −160 °C. The thermal conductivity was determined from the thermal diffusivity, the bulk density and the heat capacity of every sample. The heat capacity as a function of temperature was calculated from literature values for graphite and the corresponding carbides [7] taking into account the carbide concentration of each sample. The calculated heat capacities were compared with experimental values for doped graphites with similar dopant concentration measured by differential scanning calorimetry and reported by [8], obtaining a very good agreement.

The flexural strength, Young's modulus and strain-to-failure was measured after calcination and after graphitization by a three-point bending test on three beam specimens of every material.

The critical stress intensity factor, K_{IC}, of every material as a mass of its fracture toughness was measured by the Vickers indentation toughness test [9] using the equation proposed by Anstis et al. [10] assuming a Vickers indent radial-median crack system as fracture model. The validity of this assumption for our samples was proved experimentally [11]. This method has become widespread for brittle materials because it is simple and quick, and the specimen preparation requires only the provision of a polished surface. However, the observation of the indentation impressions with the optical and electron microscope revealed for our samples the presence of transverse cracks at the indentation faces. These cracks spend energy, which get lost for crack propagation, probably resulting in an overestimation of the K_{IC} value measured at this way. Nevertheless, this method allows in our case a comparison between all investigated materials. The test was performed on three samples of every material; five indentations were made on every sample.

To calibrate the K_{IC} values obtained by indentation, a three-point bending test with a specimen pre-cracked by Vickers indentation was performed on three beam specimens of one material (the TiC-doped sample after calcination). The K_{IC} is determined from the fracture stress and the initial crack length [12].

In order to identify the mechanisms affecting the toughness behavior of our materials, the crack propagation was investigated on each material by scanning electron microscopy (SEM). Also the fracture surfaces after the three-point bending tests were observed by SEM to identify the defect responsible for crack initiation.

Chemical erosion measurements on some of these materials were performed at the Garching high current ion source and will be reported in [13].

3. Results and discussion

In most cases, a very homogeneous carbide distribution was obtained, which demonstrates that the mixing procedure is adequate. However, if powder mixtures were stored a relatively long time, carbide agglomerations were observed, which negatively influence the mechanical properties, as described below. It is, therefore, very important to calcine the samples immediately after mixing and molding, and to pay especial attention to every step during the mixing procedure.

The crystallite height L_c as a function of the graphitization temperature is shown in Fig. 1 for samples graphitized under the same conditions (heating rate 10 °C/min, 1 h dwell at the maximum temperature), except for the graphitization at 2900 °C (*no* dwell at T_{max}). It

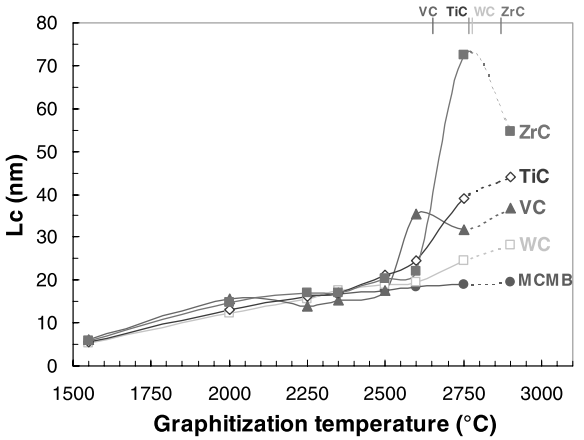

Fig. 1. Crystallite height L_c as a function of the graphitization temperature for the undoped material (MCMB) and the carbide doped samples graphitized under the same conditions (heating rate 10 °C/min, 1 h dwell at the maximum temperature), except for the graphitization at 2900 °C (no dwell at T_{max}). The temperature of the eutectics $L \leftrightarrow$ carbide + C is indicated.

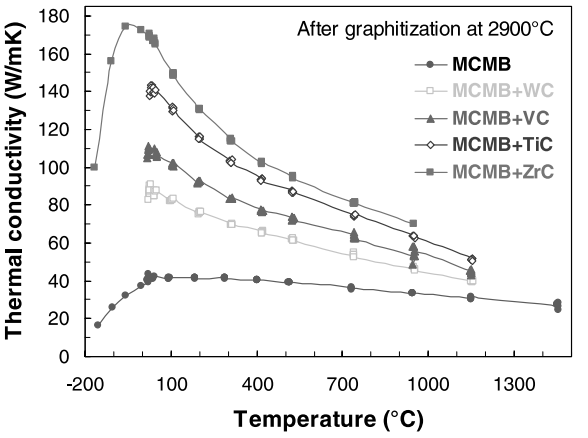

Fig. 2. Thermal conductivity as a function of temperature for samples graphitized at 2900 °C.

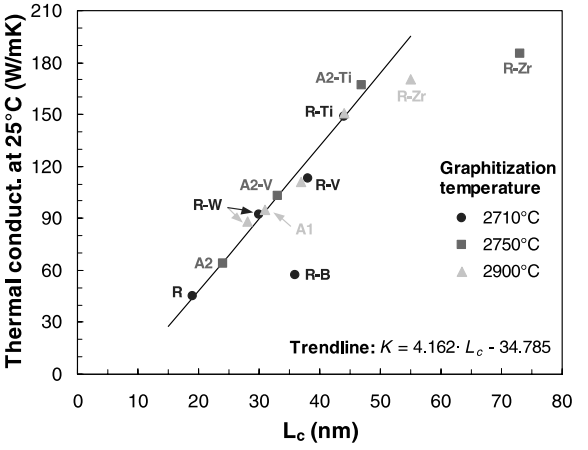

Fig. 3. Thermal conductivity at room temperature as a function of the crystallite height L_c for samples manufactured with the Repsol MCMB powder (R) and with two deliveries of MCMB powder from Alicante (A1, A2) after different graphitization cycles. The dopants are indicated behind the hyphen.

can be observed that the carbides do not act as catalyst of the graphitization below 2500 °C. VC begins to catalyze at the lowest temperature, leading to a sudden increase of L_c within a small temperature range (2500–2600 °C) which remains nearly constant with increasing temperature. ZrC seems to be the most effective catalyst, leading also to a sudden increase of L_c of a factor of ~4 as compared with the undoped material in the temperature range 2600–2750 °C. The lower L_c value of the ZrC-doped sample after graphitization at 2900 °C is probably due to the fact that there was no dwell at T_{max} for this cycle. For TiC and WC a gradual increase of L_c is observed with increasing graphitization temperature, TiC being a better catalyst than WC. In this context, one should be conscious that VC has the lowest eutectic temperature of these carbides (see Fig. 1), which may be a reason why it begins to catalyze at the lowest temperature.

The thermal conductivity of the samples graphitized at 2900 °C is shown in Fig. 2 as a function of temperature. The results are congruent with the corresponding L_c values (see Fig. 1), the ZrC sample exhibiting the highest thermal conductivity, as expected.

In order to see if there is a specific relation between the crystallite height L_c and the thermal conductivity, the room temperature value of the thermal conductivity is plotted in Fig. 3 as a function of the corresponding L_c for all samples, for which the thermal conductivity was measured up to now. There are samples of three different graphitization cycles (2710 °C with ~5 min dwell, 2750 °C with 1 h dwell, 2900 °C with no dwell) manufactured with the Repsol MCMB powder (R) and with two small deliveries of a more graphitizable MCMB powder produced at laboratory scale at the University of Alicante (A1 and A2). The dopant, if any, is indicated. One observed very clearly a linear relation for all materials with two exceptions: the B_4C-doped sample (R–B) and the two ZrC-doped samples (R–Zr) from different graphitization cycles. In the case of the B_4C-doped sample the deviation from the linear relation is easy to understand, because of the substitutional solubility of B in the graphite lattice (up to 2.35 at.% at 2350 °C [14]) leading to increased phonon scattering and thus reducing the thermal conductivity, in spite of the clear catalytic effect of B_4C.

The thermal conductivity of all grades of graphite is dominated by phonon transport along the graphite basal planes [15]. The phonon mean-free path is mainly

influenced by grain boundary scattering at low temperatures (below the maximum of thermal conductivity) and phonon scattering at higher temperatures. The improvement in thermal conductivity with increasing crystallite size is due to the larger phonon mean-free path resulting from a reduced grain boundary scattering. As Fig. 2 suggests, the maximum of thermal conductivity for our materials (except the ZrC one) seems to be close to room temperature, where grain boundary scattering dominates. Thus, it is not surprising to find a linear relation between the thermal conductivity at room temperature and the L_c value. For the ZrC-doped samples showing the largest L_c values, this maximum seems to be shifted to lower temperatures, and the room temperature thermal conductivity would be more influenced by phonon scattering, thus showing a lower thermal conductivity than predicted by the linear relation.

In Fig. 4 the open and closed porosity for the materials manufactures with the Repsol MCMB powder is shown after calcination and after graphitization at different temperatures under the same conditions. It can be observed that in the temperature range 1000–1550 °C the total porosity decreases for all samples due to solid-phase sintering during the transformation of unordered to turbostratic carbon. The smaller decrease observed for the VC- and the ZrC-doped samples is most probably due to oxygen release in this temperature range which originates additional porosity. For the case of VC, this oxygen was already present in the starting carbide powder, whereas ZrC oxidizes during calcination. For higher graphitization temperatures the total porosity of all samples remains nearly constant.

An important observation is the fact that, while for pure graphite the open and closed porosity remain constant independently of the graphitization temperature, for all doped samples the open porosity becomes gradually closed with increasing graphitization temperature. After graphitization at 2750 °C the porosity of *all* doped graphites is practically entirely closed. Taking into account that the amount of total porosity is considerable (14–19 vol.%), this phenomenon is surprising and unusual in porous ceramic materials [16]. It seems that the carbides activate a diffusion mechanism, which gradually closes the open pores. The fact that the evolution of the closed porosity with the graphitization temperature agrees with the same evolution for the L_c of every material (see Fig. 1) leads to the conclusion, that this diffusion mechanism is responsible for both the catalytic effect on the graphitization and the closing of the open porosity.

In Fig. 5 the critical stress intensity factor as measured by the Vickers indentation toughness test is shown for our materials as a function of the heat treatment temperature. As mentioned above and corroborated by the three-point bending test on pre-cracked beams of the TiC-doped material after calcination (also shown in Fig. 5), these values are overestimated. However, the K_{IC} values obtained in this way allow a comparison between some of the materials. The data shown in Fig. 5 are incomplete for some materials at high graphitization temperatures. For these materials the transverse cracks formed at the indentation faces obliged to increase the load to produce visible radial cracks; in some cases, the maximum available load was not enough to produce measurable cracks, and in other cases the sudden surface cracking of the indented area prevented the measurement of a reliable crack length.

The SEM observations of the crack propagation on every material help to understand the results shown in Fig. 5. These observations can be summarized as follows [11]:

- Crack propagation in all materials occurs by the connection of pores. Pores with high aspect ratio relieve

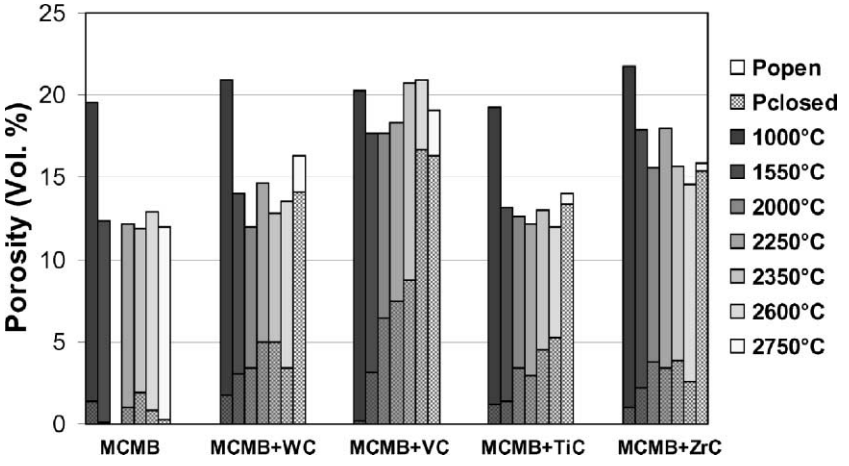

Fig. 4. Open and closed porosity for samples graphitized at different temperatures under the same conditions (10°/min, 1 h dwell).

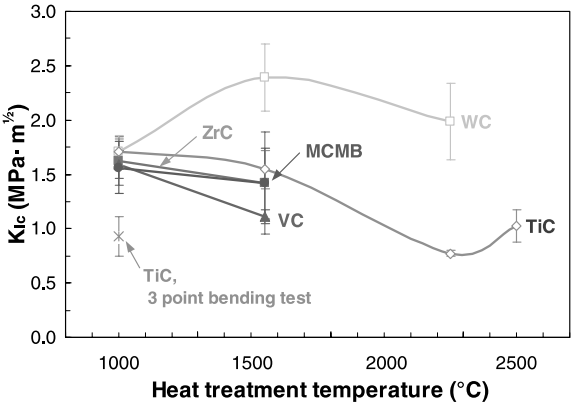

Fig. 5. Critical stress intensity factor K_{IC} measured by the Vickers indentation toughness test as a function of the graphitization temperature. The K_{IC} of the TiC-doped material after calcination as determined by a three-point bending test on precracked beams is also shown.

crack propagation, whereas larger and more equiaxed pores contributes to arrest the crack at the end of its path.

- Carbides have a double influence on crack propagation. On the one hand they compel the crack to deviate from its way because of their higher toughness compared to graphite. On the other hand the crack tends to propagate through the interface carbide–graphite indicating a weakness of this interface. This is probably due to tensile stresses originated during cooling because of the different thermal expansion coefficients of the carbides ($5.2–7.4 \times 10^{-6}$ K^{-1} between 20 and 1000 °C [17]) compared to isotropic fine-grain graphite ($\sim 4.5 \times 10^{-6}$ K^{-1} between 20 and 1000 °C [18]).

No difference in toughness is observed in Fig. 5 for the materials after calcination. After graphitization at 1550 °C the K_{IC} decreases for all materials except for the WC-doped one. Even though densification occurs in this temperature range (Fig. 4), the exit of the small volatile rest taking place in this range may lead to a change in the morphology of porosity promoting crack propagation. The larger decrease of the K_{IC} for the VC-doped sample is likely related to the larger porosity originated by oxygen release. The K_{IC} increase of the WC-doped sample is probably due to the much finer carbide distribution compared to the other doped materials, leading to porosity with a favorable morphology to prevent crack propagation. On the other hand, the coefficient of thermal expansion of WC (5.2×10^{-6} K^{-1}) is closer to the one of graphite than the other carbides and thus less tensile stresses will originate by cooling.

In the temperature range 1550–2250 °C a decrease of K_{IC} is observed for the WC- and the TiC-doped samples (the only samples for which the K_{IC} could be measured). A possible reason is the considerable L_c increase in this temperature range (Fig. 1) which promotes crack propagation due to the formation of so-called Mrozowski cracks [19,20] or microfissures formed along the *c*-axis by thermal contraction during cooling from high graphitization temperatures. The slight K_{IC} increase observed for the TiC-doped sample in the range 2250–2500 °C could be associated with the gradual transformation of the open in closed porosity (Fig. 4), since open porosity is more favorable for crack propagation.

In Fig. 6 the flexural strength and Young's modulus are shown as a function of the heat treatment temperature. Taking into account the relatively large error bars for the flexural strength values, one can say that the behavior observed is similar to the one observed for the K_{IC} of the measured materials. This is an indication that the variation of the flexural strength with the heat treatment temperature may be controlled by the K_{IC}. For the temperatures at which dopants begin to act as catalysts (>2500 °C) the flexural strength of all doped materials is very similar to the one of the undoped material and relatively high as compared to commercial fine grain graphites [18].

The SEM observation of the fracture surfaces revealed the following facts:

- On all specimens except on three of them the fracture was initiated at one of the corners, probably due to stress accumulation during compaction. From this

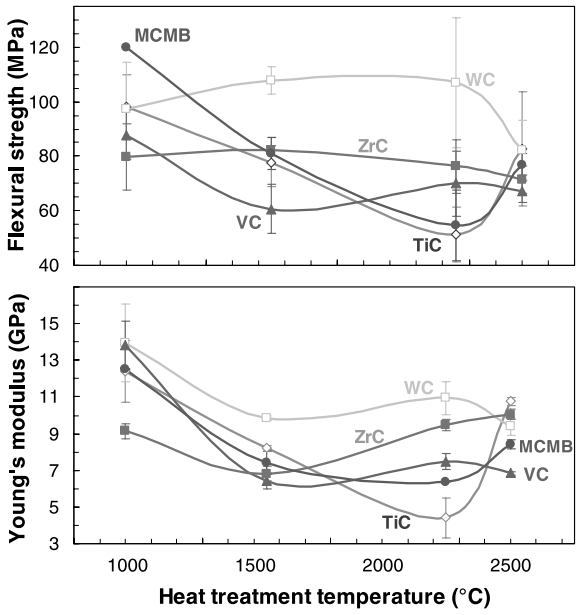

Fig. 6. Flexural strength and Young's modulus as a function of the heat treatment temperature.

it follows that the measured strength values are underestimated. In future tests the specimen corners should be chamfered to relieve stresses.

- For the three cases where the fracture was *not* initiated at the corner, the fracture was produced by carbide agglomerations, and the obtained strength value was considerably lower. This evidences the importance of a good mixing procedure of the starting powders, to obtain a homogeneous carbide distribution and to prevent agglomerations.

Concerning the Young's modulus, the tendencies are in most cases similar to them observed for the flexural strength, indicating that the Young's modulus is probably influenced by the same mechanisms as for the flexural strength and the K_{IC}. An exception is the modulus of the WC- and the ZrC-doped samples after graphitization at 1500 °C. The parameters which more influence the value of the Young's modulus are the size and morphology of the porosity [20], as well as the crystallite size (the larger L_c, the lower the Young's modulus) and the interface carbide–graphite. The observed differences are difficult to explain and probably related to a different variation of any of these parameters with the graphitization temperature.

The strain-to-failure obtained from the ratio flexural strength to Young's modulus is a mass of the thermal-shock resistance of the materials. The resulting value ranges between 0.8% and 1.5% for all materials and heat treatment temperatures. This value is considerably higher than for most commercial fine grain graphites [18] and may be probably improved by further development. If one succeeds in further improving the thermal conductivity, these materials may be very promising for the aimed application.

4. Conclusions

The conclusions of the present work can be summarized as follows:

- VC acts as catalyst at the lowest graphitization temperature, followed by TiC, WC and ZrC. This sequence is the same as for the corresponding eutectic temperature. ZrC is the most effective catalyst of the investigated carbides.
- The L_c is found to be directly proportional to the thermal conductivity at room temperature for all materials except for the B_4C-doped one, because of the B solubility in the graphite lattice, and for the ZrC-doped samples, possibly due to a larger contribution of phonon scattering.
- With increasing graphitization temperature the open porosity of all doped materials becomes gradually closed. This evolution agrees with the one observed for the L_c of these materials, suggesting that there is one and the same diffusion mechanism responsible for both the catalytic effect and the closing of the open porosity.
- K_{IC}, flexural strength and Young's modulus seems to be influenced by the same mechanisms (size and morphology of porosity, L_c, interface carbide–graphite). Differences are due to a different variation of these parameters with the graphitization temperature.
- The mechanical properties are not strongly influenced by the addition of carbides at high graphitization temperatures. The ratio flexural strength to Young's modulus, which contributes to a high thermal-shock resistance, is higher than for most commercial fine grain graphites.

Acknowledgements

We would like to thank the company REPSOL-YPF and M. Martínez Escandell (Department of Inorganic Chemistry, University of Alicante, Spain) for providing the starting mesophase carbon powders. Furthermore, the authors sincerely thank J.M. Sánchez and F. Castro (CEIT) for many helpful discussions. This work has been performed within the scope of the EFDA Technology Workprogramme 2000 (Task T438) through the EURATOM Association CIEMAT, as well as by the Spanish CICYT under grant No FTN2000-0915-C03-02. The support and encouragement of H. Bolt (IPP) and E. Hodgson (CIEMAT) is greatly acknowledged.

References

[1] J. Roth, C. García-Rosales, Nucl. Fus. 36 (1996) 1647, with corrigendum;
Nucl. Fus. 37 (1997) 897.
[2] E. Vietzke, A.A. Haasz, in: W.O. Hofer, J. Roth (Eds.), Physical Processes of the Interaction of Fusion Plasmas with Solids, Academic, San Diego, 1996, p. 135.
[3] C. García-Rosales, M. Balden, J. Nucl. Mater. 290–293 (2001) 173.
[4] A. Ōya, H. Marsh, J. Mater. Sci. 17 (1982) 309.
[5] T.B. Massalski (Ed.), Binary Alloy Phase Diagrams, vol. 1, American Society for Metals, 1986.
[6] W. Delle, K. Koizlik, H. Nickel, Graphitische Werkstoffe für den Einsatz in Kernreaktoren, Teil 2: Polykristalliner Graphit und Brennelementmatrix, Karl Thiemig Ag, Munich, 1983, p. 40.
[7] O. Knacke, O. Kubaschewski, K. Hesselmann (Eds.), Thermochemical Properties of Inorganic Substances, 2nd Ed., Springer-Verlag, Verlag Stahleisen m.b.H, Düsseldorf, 1991.
[8] B.N. Enweani, J.W. Davis, A.A. Haasz, J. Nucl. Mater. 224 (1995) 245.

[9] C.B. Ponton, R.D. Rawlings, Mater. Sci. Technol. 5 (1989) 865.
[10] G.R. Anstis, P. Chantikul, B.R. Lawn, D.B. Marshall, J. Amer. Ceram. Soc. 64 (1981) 533.
[11] E. Oyarzabal, Diploma thesis, University of Navarra, Spain, Aug. 2001.
[12] J.R. Newman, I.S. Raju, in: S.N. Atluri (Ed.), Computational Methods in Mechanics of Fracture, Elsevier Science, 1986, p. 312.
[13] M. Balden, J. Roth, C. García-Rosales, J. Nucl. Mater., in press.
[14] C.E. Lowell, J. Am. Ceram. Soc. 50 (1967) 142.
[15] B.T. Kelly, Physics of Graphite, Applied Science, 1981.
[16] I. Iturriza, F. Castro, M. Fuentes, J. Mat. Sci. 24 (1989) 2047.
[17] J. Gurland, Int. Mat. Rev. 33 (1988) 151.
[18] W. Delle, J. Linke, H. Nickel, E. Wallura, Comparison of high purity fine grain graphites from different suppliers with regard to physical, mechanical and thermal properties, Jül-Spez-401, Forschungszentrum Jülich, 1987.
[19] S. Mrozowski, Proceedings of 1st and 2nd Conferences on Carbon, 1953/1955, Waverly, Baltimore, vol. 31, 1956.
[20] B. Rand, Mechanical Properties, in: P. Delhaès (Ed.), Graphite and Precursors – World of Carbon, vol. 1, Gordon and Breach Science, 2001.